Structural characterization and SARS-CoV-2 inhibitory activity of a sulfated polysaccharide from *Caulerpa lentillifera*

Ying You [a,c], Haoran Song [b,c], Lilong Wang [b,c], Haoran Peng [d], Yujiao Sun [e], Chunqing Ai [b,c], Chengrong Wen [b,c], Beiwei Zhu [b,c,*], Shuang Song [b,c,*]

[a] College of Food Science and Engineering, Jilin Agricultural University, Changchun, PR China
[b] National Engineering Research Center of Seafood, School of Food Science and Technology, Dalian Polytechnic University, Dalian 116034, PR China
[c] National & Local Joint Engineering Laboratory for Marine Bioactive Polysaccharide Development and Application, Dalian Polytechnic University, Dalian 116034, PR China
[d] Department of Biomedical Defense, Faculty of Naval Medicine, Naval Medical University (Second Military Medical University), Shanghai 200433, PR China
[e] Natural Food Macromolecule Research Center, School of Food and Biological Engineering, Shaa-nxi University of Science and Technology, Xi'an 710021, PR China

ARTICLE INFO

ABSTRACT

Caulerpa lentillifera (Bryopsidophyceae, Chlorophyta) is an edible seaweed attracting great attention for its expansion of farming scale and increasing consumption in these years. In the present study, a sulfated poly-saccharide (CLSP-2) was isolated and separated from *C. lentillifera*, and its chemical structure was elucidated by a series of chemical and spectroscopic methods. Among these methods, mild acid hydrolysis and photocatalytic degradation were applied to release mono- and oligo-saccharide fragments which were further identified by HPLC-MS^n analysis, affording the information of the sugar sequences and the sulfate substitution in CLSP-2. Results indicated that the backbone of CLSP-2 was constructed of →6)-β-Man*p*-(1→ with sulfated branches at C2, which were comprised of prevalent →3)-β-Gal*p*4S-(1→, →3)-β-Gal*p*2,4S-(1→, and minor Xyl. In addition, the virus neutralization assay revealed that CLSP-2 could effectively protect HeLa cells against SARS-CoV-2 infection with an IC$_{50}$ of 48.48 μg/mL. Hence, the present study suggests CLSP-2 as a promising agent against SARS-CoV-2.

1. Introduction

Caulerpa lentillifera (Bryopsidophyceae, Chlorophyta) is an edible green seaweed with a grape-like appearance and a caviar-like taste, it is also known as "green caviar". *C. lentillifera* is mainly distributed in tropical and subtropical regions, such as Philippine, Vietnam, and Japan. Recently, *C. lentillifera* has received considerable attention for its expansion of farming scale and increasing consumption (Stuthmann et al., 2021). *C. lentillifera* is a low-energy food with high contents of dietary fibers, and its polysaccharide content is as high as ≥40% (dry weight) (Zhang et al., 2020). Sulfated polysaccharides isolated from *C. lentillifera* (CLSPs) have been reported to have antioxidant (Tian et al., 2019), anti-diabetic (Khairuddin et al., 2020), and anticancer activities (Maeda et al., 2012). Moreover, a homogeneous fraction, CLGP4, with the monosaccharide composition of Xyl, Man, and Gal in a percentage ratio of 1.00:2.15:2.40 and a molecular weight of 3877.8 kDa exhibited immunostimulatory effect (Sun et al., 2018; Sun et al., 2019). These researches suggest CLSPs as a health-improving ingredient, and further exploitation on CLSPs is still needed for their application in the nutra-ceutical industry.

Severe acute respiratory syndrome coronavirus-2 (SARS-CoV-2) has caused the catastrophic COVID-19 epidemic, leading to over million deaths to date. This ongoing epidemic has seriously affected public health and social stability. Enormous efforts in alleviating disease symptoms and impeding viral spread are being made. Besides the development of vaccines, the discovery of anti-virus agents is an urgent demand to prevent COVID-19. Recently, sulfated polysaccharides have earned significant attention for their effective inhibitory effects against SARS-CoV-2 (Hans et al., 2020; Kwon et al., 2020), such as heparin (Ayerbe et al., 2020), fucoidan (Song et al., 2020), and carrageenan

(Jang et al., 2021). These sulfated polysaccharides could bind to the SARS-CoV-2 spike glycoprotein, so to prevent virus entry into the host cells (Yim et al., 2021). Given that the COVID-19 epidemic is still going on, more efforts are needed to discover effective anti-virus agents against SARS-CoV-2 in the present urgent situation. In addition, the structural elucidation of the bioactive polysaccharides could promote the understanding of the structure-property relationship, which could guide the discovery of more effective inhibitor against SARS-CoV-2.

In the present study, a novel sulfated polysaccharide CLSP-2 was isolated from *C. lentillifera* by hot water extraction and purified by column chromatography. Its structure was elucidated by a combination of chemical and spectroscopic methods. Moreover, the virus neutralization assay was conducted by using the indirect immunofluorescent method. The finding in the present study could enlarge the knowledge of *C. lentillifera* resource, and promote its application as the functional ingredients or nutraceuticals in the food and medical industry.

2. Materials and methods

2.1. Materials and chemicals

Fresh green seaweed *C. lentillifera* was purchased from Nha Trang, Khanh Hoa province, Vietnam. Trifluoroacetic acid (TFA, Guangfu precise chemical institute, Tianjin, China), 1-phenyl-3-methyl-5-pyrazolone (PMP, Sinopharm Chemical Reagents Co., Beijing, China), TiO_2, H_2O_2, CH_3I, and NaOH were all analytical grade reagents (Damao chemical reagent factory, Tianjin, China). Acetonitrile and dichloromethane (Fisher, Pittsburgh, Pennsylvania, USA) were HPLC grade reagents.

2.2. Preparation of CLSP-2

Fresh *C. lentillifera* (1000 g) was washed with tap water and homogenized. The homogenate was heated at 90 °C for 2 h and then centrifuged at 3500*g* for 20 min. Then the distilled water (1000 mL) was added to the precipitate to repeat the extraction procedure. After that, all the supernatants were combined, concentrated, and precipitated with a 4-fold volume of ethanol for 12 h at 4 °C. The resulting precipitate was re-dissolved in deionized water. Protein was removed by using Sevag's method and the solution was dialyzed, concentrated, and lyophilized to obtain the crude polysaccharide (CLP). CLP was sequentially purified by anion exchange chromatography and ultrafiltration. Briefly, CLP (1 g) was dissolved in distilled water (20 mL) and loaded onto a DEAE-cellulose-52 column (4.0 cm × 60 cm), which was sequentially eluted with 0.5 M, 0.8 M, and 1.2 M NaCl solutions, and 3 fractions were obtained after dialysis and lyophilization, namely CLP-1, CLP-2, and CLP-3. CLP-2 was further purified by using 50 mL Millipore ultrafiltration tube (molecular weight cut-off, MWCO: 100 kDa). The retentate was collected and named as CLSP-2.

2.3. Chemical composition analysis of CLSP-2

The neutral sugar content of CLSP-2 was determined using the phenol-sulfuric acid method with galactose as a standard. The contents of protein, sulfate and uronic acid were measured with Braford method, barium chloride gelatin method and carbazole-sulfuric acid method, respectively. All experiments were repeated three times.

2.4. Monosaccharide composition analysis of CLSP-2

Monosaccharide composition of CLSP-2 was analyzed according to our previous method (H. X. Wang et al., 2015). Briefly, CLSP-2 was hydrolyzed with 2.0 M TFA at 121 °C for 3 h, and the resulting solution was dried by nitrogen and labeled with PMP. Then, the PMP derivatives were analyzed by HPLC. A Diamosil C18 column (250 mm × 4.6 mm, 5 μm, Dikma Technologies Inc., Beijing, China) and a photodiode array

(PDA) detector were applied, which controlled by XCalibur software (Thermo Fisher Scientific, Basel, Switzerland). The column temperature was 35 °C and the mobile phase was 20 mM ammonium acetate (A) and acetonitrile (B) (A:B = 78:22, v/v) with a flow rate of 1.0 mL/min. Experiment was repeated three times.

2.5. Microscopes

Atomic force microscope (AFM5500, Japan) was used to obtain the images of CLSP-2 in tapping mode. CLSP-2 was dissolved in distilled water to get a final concentration of 10 μg/mL. A 10 μL drop was pipetted onto freshly cleaved mica and dried at room temperature to capture the images.

The transmission electron microscopy (TEM) of CLSP-2 was performed using a JEM-2100 electron microscope (JEOL, Japan). The CLSP-2 solution (1 mg/mL) was dip-coated on a 300-mesh copper grid coated with a carbon film and dried at room temperature to capture the images.

2.6. Molecular weight determination

The relative molecular weight of CLSP-2 was determined by high performance gel permeation chromatography (HPGPC). An analytical column of TSK-G5000PWXL (7.8 mm × 300 mm) equipped with a refractive index detector (Waters 2414, USA) was used. The mobile phase was 0.1 M ammonium acetate at a flow rate of 0.6 mL/min. Dextrans (Sigma, USA) with molecular weights of 5, 12, 25, 50, 150, 410, and 670 kDa were used as standard polysaccharides.

2.7. Mild acid hydrolysis

CLP (100 mg) was infiltrated with 0.2 M TFA in a sealed tube and kept at 105 °C for 1 h. Then the resulting solution was centrifuged at 3000*g* for 15 min after cooled to room temperature. The precipitate was collected and dissolved in 2.0 M TFA at 121 °C for monosaccharide composition analysis according to Section 2.4. A portion of the supernatant was directly labeled with PMP for oligosaccharide analysis, while another portion was fully hydrolyzed with 2.0 M TFA at 121 °C followed by Section 2.4.

2.8. Photocatalytic degradation of CLSP-2

The photocatalytic reaction was carried out in a Photocatalytic Xenon Light Source System (CEL-HXF300-T3, Zhongjiao Jinyuan Technology Co., Beijing, China) with a 300 W Xenon lamp (Xenon lamp 300 W, PerkinElmer). Briefly, CLSP-2 (50 mg) was dissolved in 10 mL distilled water and TiO_2 (50 mg) was added into the solution. The light was turned on to initiate the reaction after the addition of H_2O_2 (0.19 mL). During the photolysis experiment, the solution was placed in the reactor and stirred magnetically with simultaneous exposure to Xenon light and the illumination time was 20 min. After that, the solution was centrifuged at 10,000*g* for 10 min and the supernatant solution was collected for HPLC-PDA-MS^n analysis.

2.9. HPLC-PDA-MS^n analysis

After PMP derivation (Section 2.4), the products of acid hydrolysis and photocatalytic degradation were analyzed by a LXQ linear ion trap mass spectrometer equipped with an electrospray ion source (ESI) and a PDA detector, controlled by XCalibur software (Thermo Fisher Scientific, Basel, Switzerland). The ESI-MS settings were set as we previously reported (Song et al., 2018). Data were acquired in positive mode (for acid hydrolysis samples) or negative mode (for photocatalytic degradation samples), and the scan range was set from *m/z* 100 to 2000 am. A TSKgel-Amide-80 (4.6 mm × 150 mm, 3 μm) column was used, the column temperature was 35 °C, and the mobile phase consisted of 20 mM ammonium acetate-acetonitrile (78:22, v/v, pH = 6.0) with a flow
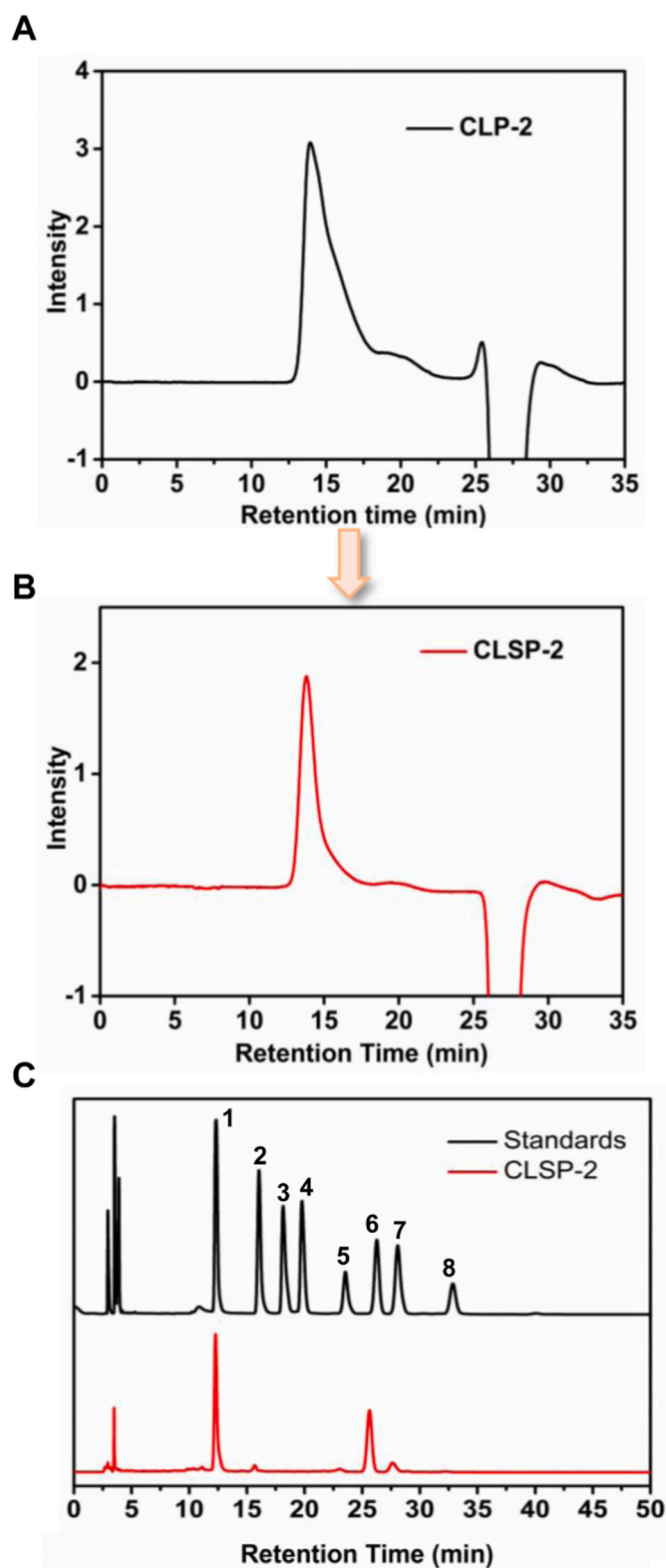
Fig. 1. The chromatograms of CLSP-2 before (A) and after (B) purification, and (C) HPLC profiles of monosaccharide composition of CLSP-2. Monosaccharide standards: 1: Mannose, 2: Rhamnose, 3: Glucuronic acid, 4: Galacturonic acid, 5: Glucose, 6: Galactose, 7: Xylose, and 8: Fucose.

rate of 0.2 mL/min.

2.10. Desulfation of CLSP-2

Desulfation of CLSP-2 was performed using DMSO-methanol method after the preparation of CLSP-2 pyridinium salt (Song et al., 2018). Briefly, CLSP-2 (100 mg) was dialyzed against 0.1 M pyridine hydrochloride solution and lyophilized to obtain the pyridinium salt. Then, the pyridinium salt (85 mg) was dissolved in dimethyl sulfoxide: methanol: pyridine = 87:10:3 (v/v/v) at 100 °C for 6 h. After that, the solution was dialyzed against deionized water and lyophilized. The desulfated product was named as dS-CLSP-2.

2.11. Fourier transform-infrared (FT-IR) spectroscopy

CLSP-2 (2 mg) and dS-CLSP-2 (2 mg) were individually mixed and grounded with 100 mg KBr, and then punched into 1 mm pellets for analysis in the frequency of 400 to 4000 cm^{-1} on a Spectrum One-B FTIR Spectrometer (Perkin, USA).

2.12. NMR spectroscopic analysis

CLSP-2 (30 mg) and dS-CLSP-2 (30 mg) were individually dissolved in 500 μL D_2O (99.9%), and exchangeable proton was substituted by deuterium after lyophilization for three times. Their ^1H NMR, ^{13}C DEPT135 NMR, heteronuclear single quantum correlation (HSQC), ^1H—^1H correlation spectroscopy (^1H—^1H COSY), ^1H—^1H nuclear overhauser effect spectroscopy (NOESY), and total correlation spectroscopy (TOCSY) were recorded on a Bruker Acsend 400 spectrometer (Bruker, German).

2.13. Methylation and GC–MS analysis

CLSP-2 and dS-CLSP-2 were methylated as previously described (Hakomori, 1964; Ken-ichi et al., 1997) with minor modification. Firstly, CLSP-2 was transferred to triethylamine-salt (t-CLSP-2) form. Then t-CLSP-2 and dS-CLSP-2 were methylated by Needs and Selvendran method (Needs & Selvendran, 2010). After that, the methylated samples were hydrolyzed, reduced, and acetylated to convert into their partially methylated alditol acetates. These derivatives were analyzed by GC–MS, which was performed on a Shimadzu GCMS-2010 system equipped with an electron impact ion source (ionization energy 70 eV) and a Rtx-5MS capillary column (0.25 mm × 30 m, 0.25 μm).

2.14. Determination of absolute configuration

The absolute configuration of Gal in CLSP-2 was determined according to previously reported method with minor modification (Tanaka et al., 2007). Briefly, CLSP-2 was hydrolyzed with 2.0 M TFA at 121 °C for 3 h, and the resulting solution was dried by nitrogen. Then, the dried hydrolyzed product, L-Gal, and D-Gal were dissolved in pyridine respectively. After that, L-cysteine methyl ester hydrochloride was added and heated at 60 °C for 1 h, and then *o*-tolyl isothiocyanate was added in these mixtures and heated at 60 °C for 1 h. The reaction mixtures were analyzed by HPLC. A Diamosil C18 column (250 mm × 4.6 mm, 5 μm, Dikma Technologies Inc., Beijing, China) and a PDA detector were applied. The column temperature was 35 °C and the mobile phase was water (A) and acetonitrile (B) (A:B = 79:21, v/v) with a flow rate of 0.8 mL/min.

2.15. Virus neutralization assay

The assay was carried out according to our previously reported method (Song et al., 2020) in a biological safety protection third-level laboratory of Naval Medical University. Briefly, HeLa cells were seeded in 96-well plates and incubated for 12 h. Then, the solution of
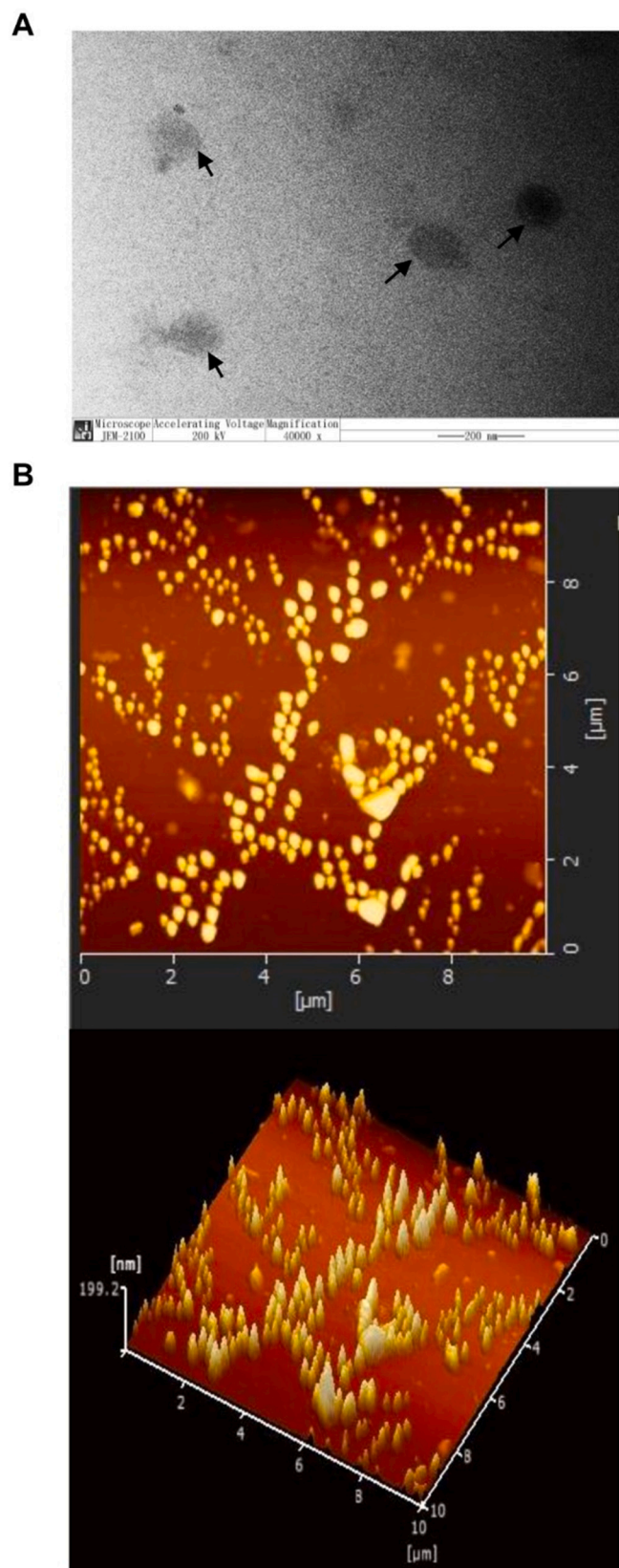
Fig. 2. TEM micrograph (A) and AFM images (B) of CLSP-2 dissolved in water.
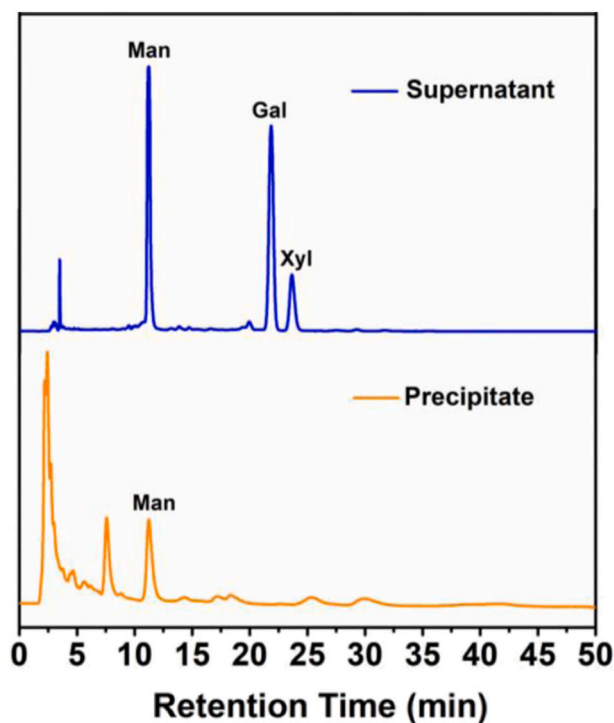

Fig. 3. Monosaccharide composition analysis of mild acid hydrolysis products derivatized with 1-phenyl-3-methyl-5-pyrazolone.

different concentrations of CLSP-2 and the SARS-CoV-2 virus were mixed equally to replace the medium in the well and infect HeLa cells. After incubation for 24 h, the indirect immunofluorescent assay was carried out, and images were captured using Cytation 5 Imaging Reader (BioTek, USA).

2.16. Statistical analysis

All the results were presented as mean $\pm$ SD. Data were analyzed using one-way ANOVA multiple-comparisons tests by Prism 7.0. Differences between the groups were considered statistically significant at $p < 0.05$.

3. Results and discussion

3.1. Chemical composition and morphology of CLSP-2

The crude polysaccharide (CLP) was obtained from fresh *C. lentillifera* by hot-water extraction, ethanol precipitation and, protein removal, and then it was subjected to a DEAE-cellulose-52 column to afford 3 fractions. The major fraction (CLP-2, Fig. 1A) was further purified by using ultrafiltration (MWCO: 100 kDa), and the resulting retentate (CLSP-2) showed a single narrow peak in HPGPC (Fig. 1B). The neutral sugar content of CLSP-2 was 70.82% $\pm$ 1.60% and its protein content was as low as 1.86% $\pm$ 0.02%. A high sulfate content (22.72% $\pm$ 0.42%) and a low uronic acid content (1.65% $\pm$ 0.18%) were found in CLSP-2. Furthermore, 3 component monosaccharides including Gal, Man, and Xyl were identified (Fig. 1C) and their contents were 48.9%, 40.0%, and 11.1%, respectively. The morphology of CLSP-2 in water was characterized by TEM and AFM. Spherical particles with the varying radius distribution (around 200 nm) could be observed in both TEM (Fig. 2A) and AFM (Fig. 2B).

In addition, the average molecular weight of CLSP-2 was estimated to be 3985 kDa, which is quite high for a natural polysaccharide. Nirmal Pugh et al. isolated 3 polysaccharides with the molecular weight above 10^4 kDa from *Spirulina platensis*, *Aphanizomenon flos-aquae* and *Chlorella*
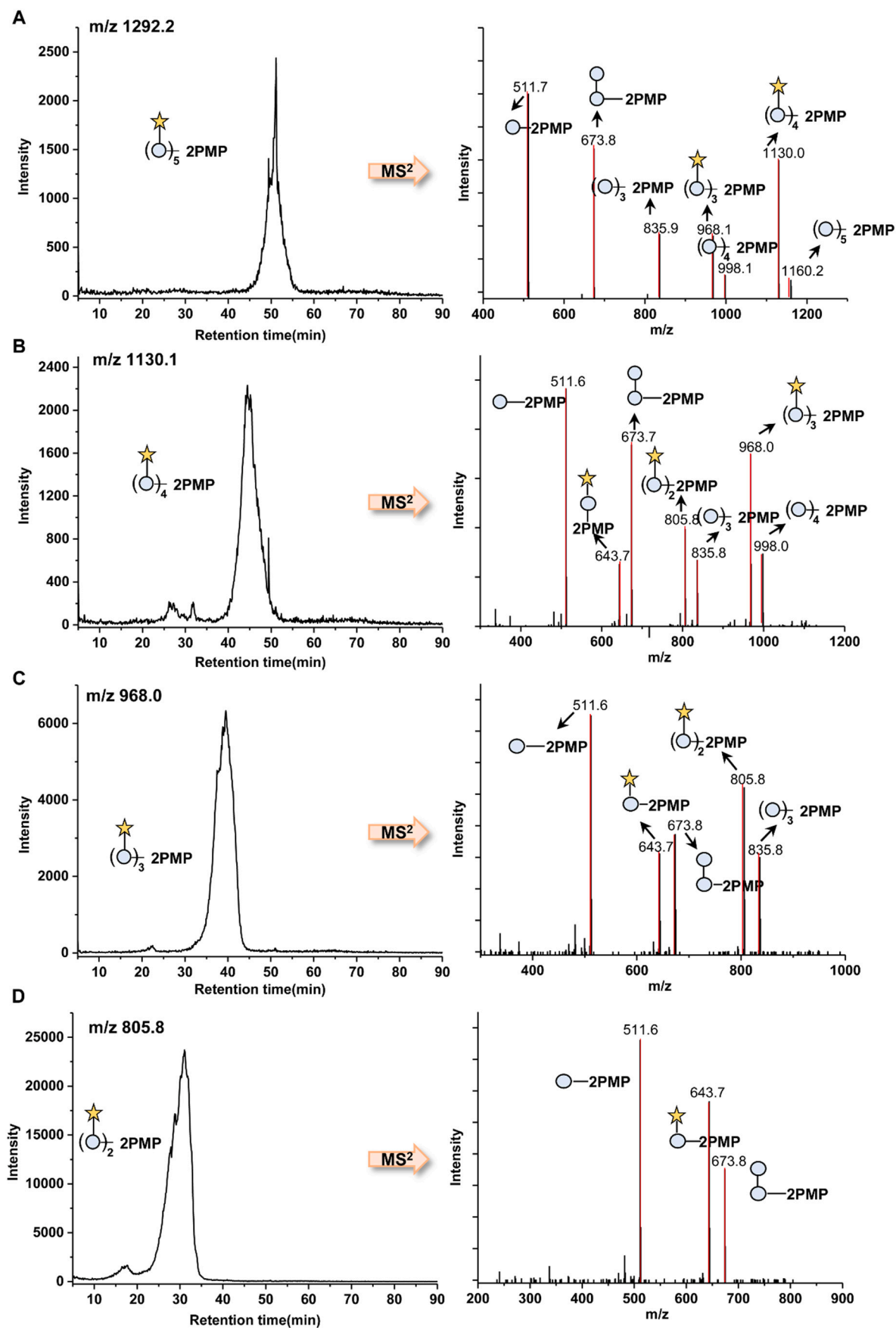
Fig. 4. HPLC-MS^n analysis results of representative oligosaccharide fragments from mild acid hydrolysis. Hexasaccharide: Xyl → (Hex)$_5$ (A), pentasaccharides: Xyl → (Hex)$_4$ (B), tetrasaccharides: Xyl → (Hex)$_3$ (C), and trisaccharides: Xyl → (Hex)$_2$ (D). The blue circle (◯) represents Hex, and the pentagram (☆) stands for Xyl.
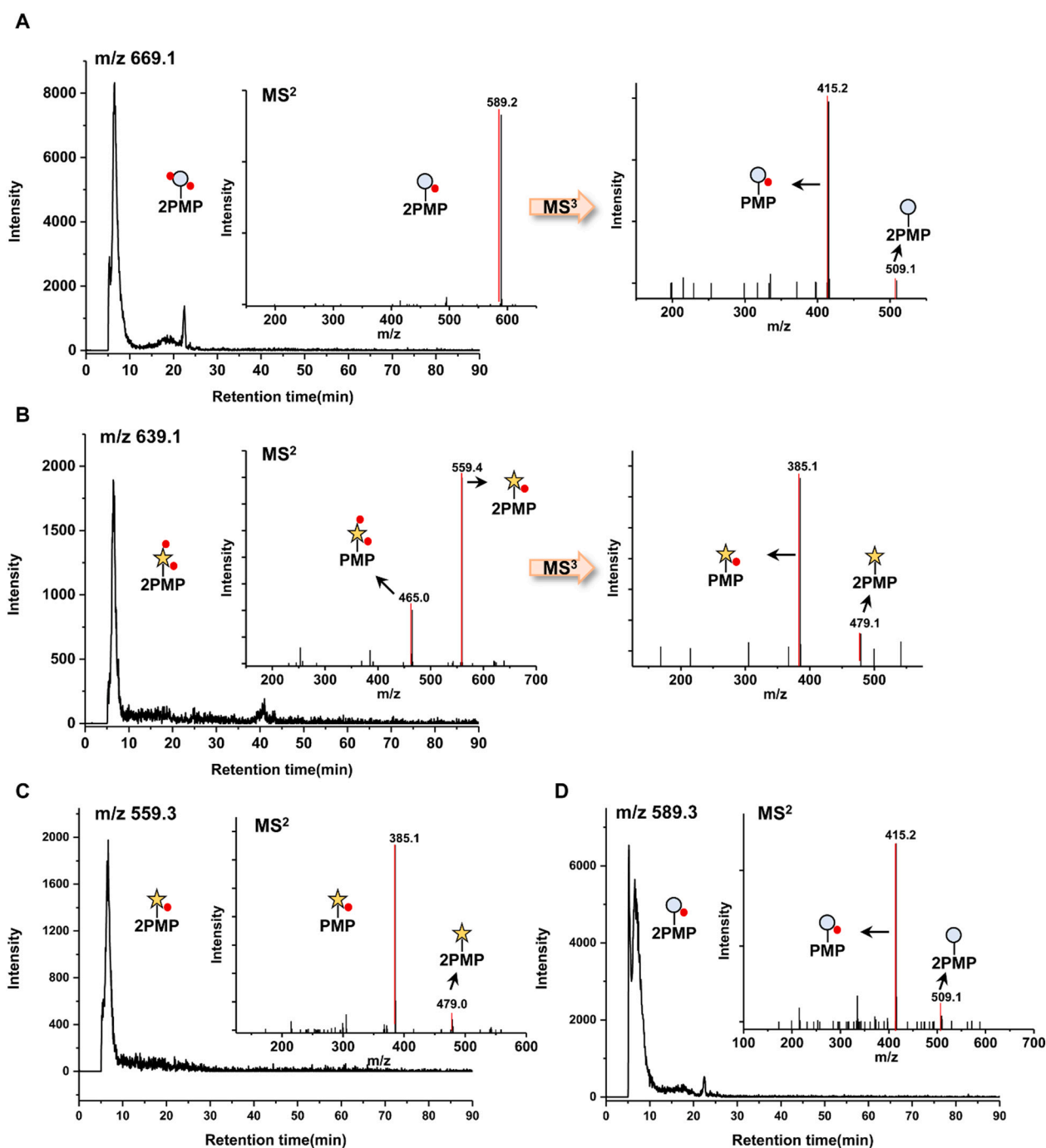
Fig. 5. HPLC-MS^n analysis results of representative fragments from photocatalytic degradation. Hexose residue with di-sulfate groups (A), Xyl residue with di-sulfate groups (B), Xyl residue with mono-sulfate group (C), and hexose residue with mono-sulfate group (D). The blue circle (○) represents Hex, the pentagram (☆) stands for Xyl, and the red small circle (●) stands for sulfate group.

pyrenoidosa (Pugh et al., 2001), while polysaccharide from red alga *Coccotylus truncatus* was also reported to have the higher molecular weight about 10^3 kDa (Tuvikene et al., 2009). Therefore, it is common to have the high molecular weight polysaccharides in marine alga.

3.2. Analysis on the products of acid hydrolysis and photocatalytic degradation

In order to further explore the composition of CLSP-2, acid hydrolysis and photocatalytic degradation were carried out, and their products were derivatized by PMP before HPLC-MS^n analysis. The mild acid hydrolysis followed by centrifugation was conducted to separate the core (precipitate) and branches (supernatant) of CLSP-2. Then further full acid hydrolysis of the precipitate and the supernatant demonstrated that the core of CLSP-2 was composed of mannose while the branch chains mainly contained galactose and xylose (Fig. 3A). The PMP derivatives of oligosaccharide fragments in the supernatant were characterized by their mass spectra and retention times on the hydrophilic interaction chromatography. Thus, hexasaccharides ((Hex)$_6$, Xyl → (Hex)$_5$, and (Xyl)$_2$ → (Hex)$_4$), pentasaccharides ((Hex)$_5$, Xyl → (Hex)$_4$, and (Xyl)$_2$ → (Hex)$_3$), tetrasaccharides ((Hex)$_4$, Xyl → (Hex)$_3$, (Xyl)$_2$ → (Hex)$_2$, and (Xyl)$_3$ → Hex), trisaccharides ((Xyl)$_2$ → Hex or Hex→(Xyl)$_2$, Xyl → (Hex)$_2$, (Hex)$_3$), and disaccharides (galobiose, Xyl → Hex, and Xylobiose) were identified in the supernatant after acid hydrolysis
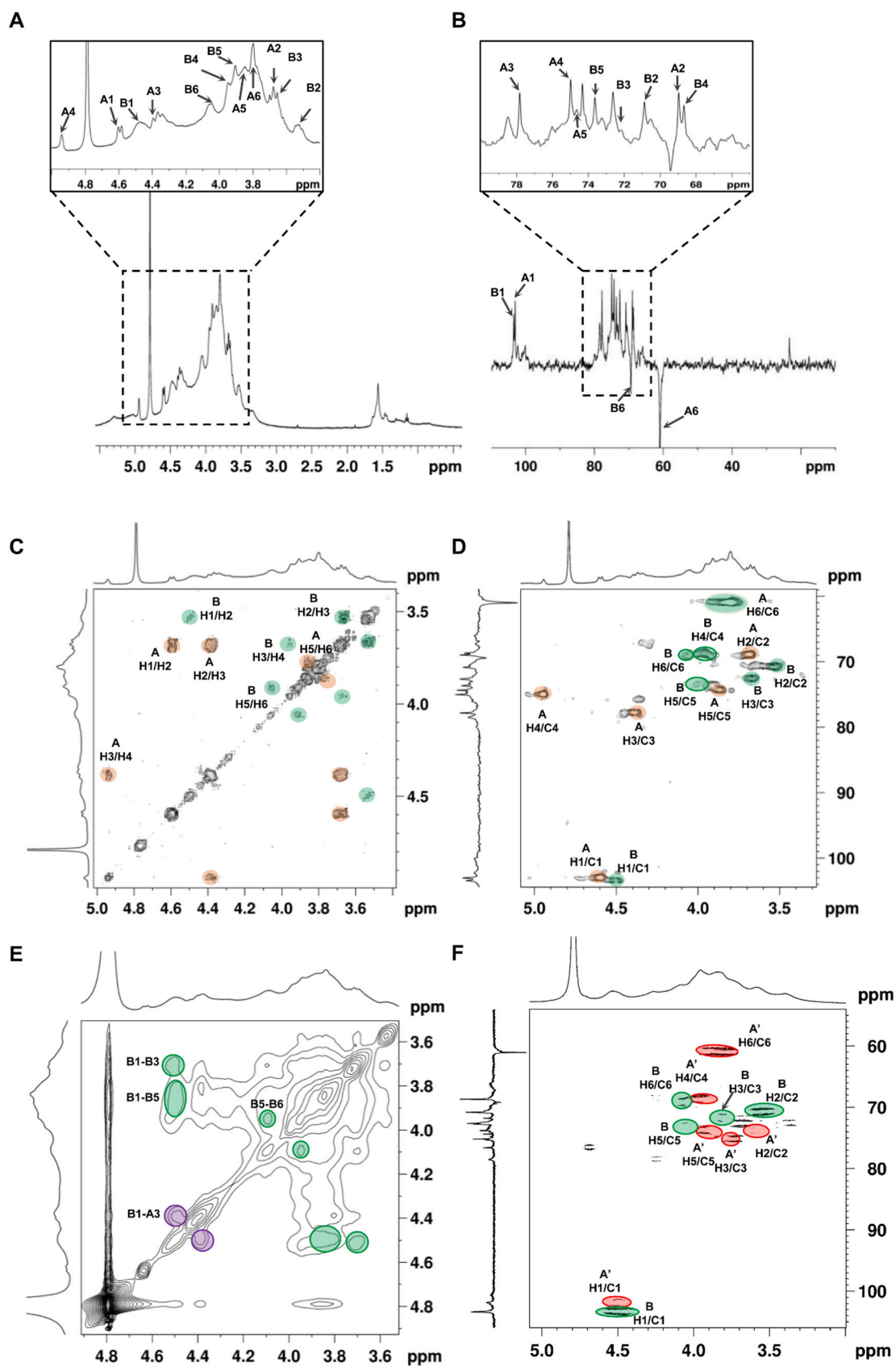
Fig. 6. ^{1}H NMR (A), ^{13}C DEPT135 NMR (B), [1]H—^{1}H COSY (C), HSQC (D), and NOSEY (E) spectra of CLSP-2, and HSQC (F) spectrum of dS-CLSP-2.

Table 1
^{1}H and ^{13}C NMR chemical shifts of CLSP-2 and dS-CLSP-2 in D$_2$O.

Sample	Glycosyl residues	^{13}C/^{1}H (ppm)					
		C1/H1	C2/H2	C3/H3	C4/H4	C5/H5	C6/H6
CLSP-2	A: →3)-β-D-Galp4S-(1→	103.1/4.61	68.8/3.70	77.7/4.40	74.9/4.95	73.4/3.89	60.7/3.80
	B: →6)-β-Manp-(1→	103.4/4.51	70.8/3.55	72.5/3.68	68.7/3.97	73.6/3.93	68.8/4.07
dS-CLSP-2	A′: →3)-β-D-Galp4diS-(1→	101.9/4.49	70.6/3.58	75.0/3.79	68.6/3.97	73.7/3.92	60.9/3.83
	B: →6)-β-Manp-(1→	103.2/4.51	70.8/3.55	71.5/3.82	68.3/3.98	73.6/3.96	68.7/4.09

Table 2
Results of methylation analysis of CLSP-2 and dS-CLSP-2.

Retention time (min)	Methylated derivative	Deduced linkage	Characteristic fragments (*m/z*)	Molar ratio	
				CLSP-2	dS-CLSP-2
11.21	2,3,4-Me$_3$-Man	→6)-β-Manp-(1→	99, 113, 117, 129, 161, 173, 189, 233	2.3	2.1
12.14	2,6-Me$_2$-Gal	→3,4)-β-Galp-(1→	87, 117, 129, 159, 245, 261	2.5	0.9
14.52	3,4-Me$_2$-Man	→2,6)-β-Manp-(1→	87, 99, 113, 129, 173, 189, 233	1.0	1.0
22.69	6-Me-Gal	→2,3,4)-β-Galp-(1→	73, 129, 139, 145, 157, 217, 259, 289	0.7	/
9.95	2,4,6-Me$_3$-Gal	→3)-β-Galp-(1→	71, 87, 101, 117, 129, 161, 173, 233	/	1.9

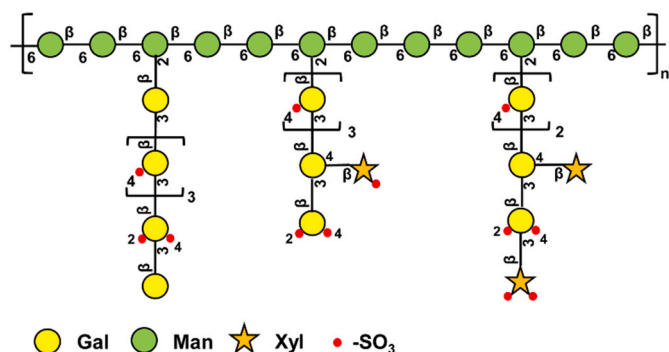○ Gal ● Man ☆ Xyl • -SO$_3$

Fig. 7. The proposed structure of CLSP-2.

(Figs. 4 and S1, S2, and S3). Furthermore, the oligosaccharide fragments such as hexobiose and xylobiose with or without a sulfate group as well as xylotriose with a sulfate group were detected in the photocatalytic reaction solution (Figs. S4 and S5). It is worth mentioning that the hexose residue with mono- or di- sulfate groups (Fig. 5A and D), and the xylose with mono- or di- sulfate groups (Fig. 5B and C) were also observed, indicating the sulfate substitution of hexose and Xyl residues.

The acid hydrolysis results indicate that the CLSP-2 is a cell-wall polysaccharide of *C. lentillifera* with mannan as the backbone and the Gal, Xyl as the component monosaccharides in branch chains, and it has been reported that mannan is the main cell-wall polysaccharide in green alga (Fernández et al., 2012; Kaihou et al., 1993). Kinds of oligosaccharide fragments were observed after the mild acid hydrolysis, but of note, the small oligosaccharide fragments may be the degradation products of the large fragments. Thus, (Hex)$_6$, Xyl → (Hex)$_5$, and (Xyl)$_2$ → (Hex)$_4$ are proposed as the major branches in CLSP-2. However, acid hydrolysis could remove the sulfate group while the radical oxidation degradation can break polysaccharides down without serious desulfation (Yun et al., 2012). As a type of radical oxidation degradation

methods, the photocatalytic degradation showed great advantage to provide the information of sulfate substitution in the present study, which proved the existence of mono- or di- sulfated substitution of hexose (Gal or Man) and Xyl residues.

3.3. FT-IR and NMR analysis of CLSP-2 and dS-CLSP-2

The structure of CLSP-2 was further elucidated with FT-IR and NMR spectroscopy and methylation analysis by comparing with its desulfated derivative, dS-CLSP-2. In FT-IR spectra (Fig. S6), the bands around 1258 cm^{-1} and 826 cm^{-1} were caused by the stretching vibration of S=O and C-O-S, respectively, which are typical for sulfated polysaccharides (J. Wang et al., 2010). Then these S=O and C-O-S stretching vibration bands were disappeared in the FT-IR spectrum of dS-CLSP-2 due to the desulfation. In addition, the band at 1642 cm^{-1} could be attributed to the carboxylic groups bound with hydrogen bonds. In dS-CLSP-2, due to the missing of sulfate group, their hydrogen bonds with the carboxylic groups were broken, so some carboxylic acid ester groups showed the band near 1740 cm^{-1}.

The ^{1}H NMR, ^{13}C DEPT135 NMR, ^{1}H—^{1}H COSY, HSQC, TOCSY, and NOESY spectra were applied to elucidate the structure of CLSP-2. In the HSQC spectrum of CLSP-2, the cross peaks at 4.61/103.1 ppm (residue A) and 4.51/103.4 ppm (residue B) were identified as the anomeric proton/carbon signals (Fig. 6D). The ^{1}H—^{1}H COSY spectrum showed the clear vicinal coupling correlations of A-H1 (4.61 ppm) with A-H2 (3.70 ppm), A-H2 with A-H3 (4.40 ppm), A-H3 with A-H4 (4.95 ppm), and B—H1 (4.51 ppm) with B—H2 (3.55 ppm), B—H2 with B—H3 (3.68 ppm), and B—H3 with B—H4 (3.97 ppm). Moreover, the vicinal coupling correlation of B—H5 (3.93 ppm) with B—H6 (4.07 ppm) was also observed in ^{1}H—^{1}H COSY spectrum. Then, the directly bonded carbons of these protons were assigned individually by HSQC spectroscopy. The inverted peaks of 60.7 ppm and 68.8 ppm in ^{13}C DEPT135 NMR spectrum (Fig. 6B) were assigned as C6 of residue B and residue A, respectively. The directly bonded protons of A-C6 were assigned by HSQC spectrum and the vicinal coupling correlation of A-H5 (3.89 ppm) with A-H6 (3.80 ppm) was observed in ^{1}H—^{1}H COSY spectrum. The assignment of protons and carbons of CLSP-2 (Table 1) was also confirmed by TOCSY spectrum (Fig. S6A).

In addition, ^{1}H NMR, ^{13}C DEPT135 NMR, ^{1}H—^{1}H COSY, and HSQC spectra were used for dS-CLSP-2 structural analysis. The signals for residue B were also observed in the NMR spectra of dS-CLSP-2 while the new cross peak of 4.61/103.1 ppm in the HSQC spectrum (Fig. 6F) suggests the existence of desulfated of residue A, named as residue A′. Then, all the chemical shifts of protons and carbons in dS-CLSP-2 (Table 1) were assigned based on the analysis of the ^{1}H—^{1}H COSY (Fig. S7) and HSQC (Fig. 6F) spectra of dS-CLSP-2.

By comparing ^{1}H and ^{13}C chemical shifts of those in literature reports (Lu et al., 2010; H. X. Wang et al., 2015), the A′ residue in dS-CLSP-2 was then determined as →3)-β-Galp-(1→, and A residue in CLSP-2 was assigned as →3)-β-Gal-(1→ with a lower field shift (74.9 ppm) at C4, indicting the sulfate substitution at C4 of Gal. In addition, the absolute configuration of Gal was determined. The result showed that the retention time of Gal in CLSP-2 was same as the standard D-Gal (Fig. S8), indicating the D absolute configuration of Gal. The lower field shift (68.9 ppm) of B residue suggests the glycosidic linkage at C6, and then the B residue was identified as →6)-β-Manp-(1→ by comparing its NMR
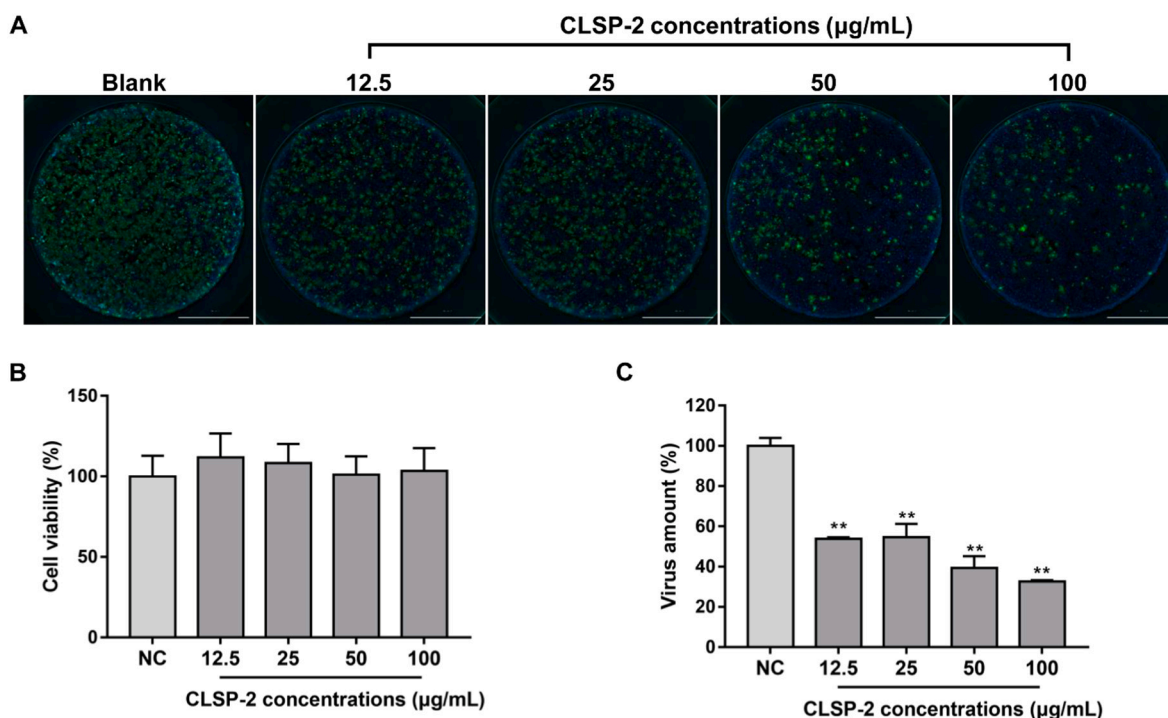
Fig. 8. Inhibitory activity of CLSP-2 against SARS-CoV-2. Representative images of immunofluorescent assay of CLSP-2 (A), relative virus amount of CLSP-2 at different concentrations (B), cell viability of CLSP-2 on HeLa cells (C). Data were presented as mean ± SD ($n = 3$). Significant effect between different groups: **$p < 0.01$.

data with those reported previously (Alban et al., 2002; Song et al., 2018; Zdorovenko et al., 2017). The unassigned signals in the NMR spectra (Figs. 6 and S7) were most likely from xylose and 2,6-linked mannose units which were observed in the HPLC-MS analysis after degradation (Section 3.2) and methylation analysis (Section 3.4). However, because of the serious overlap of the NMR signals as well as the relative low proportions of xylose and 2,6-linked mannose units, it is greatly difficult to assign their NMR signals.

3.4. Methylation analysis of CLSP-2 and dS-CLSP-2

Further methylation analysis revealed the linkage pattern of CLSP-2 and dS-CLSP-2 as shown in Table 2. Compared to those of CLSP-2, obvious decreases of →3,4)-β-Gal*p*-(1→ and →2,3,4)-β-Gal*p*-(1→ as well as an increase of →3)-β-Gal*p*-(1→ were observed in dS-CLSP-2, indicating the sulfate substitution at C4 or both C2 and C4 of Gal residue. Meanwhile, the molar ratios of →6)-β-Man*p*-(1→ and →2,6)-β-Man*p*-(1→ in dS-CLSP-2 were similar to those in CLSP-2, suggesting no sulfate substitution at the Man residue.

The residue of →3)-β-Gal*p*-(1→ with a sulfate group at C4 was also identified in the NMR analysis, and the →3)-β-Gal*p*2,4S-(1→ residue found in methylation analysis was in line with the identification of the di-sulfated hexose observed in photocatalytic degradation products. Since Man had been deduced as the backbone component based on acid hydrolysis results, further methylation analysis indicated the backbone of CLSP-2 was composed of →6)-β-Man*p*-(1→ with branches at C2. Thus, it could be proposed that the backbone of CLSP-2 was constructed of →6)-β-Man*p*-(1→ with sulfated branches comprised of prevalent →3)-β-Gal*p*4S-(1→, →3)-β-Gal*p*2,4S-(1→, and minor Xyl (Fig. 7).

3.5. Inhibitory effect of CLSP-2 against SARS-CoV-2

The effect of CLSP-2 against SARS-CoV-2 was determined, and the representative images of immunofluorescent assay are shown in Fig. 8A. In addition, the effect of CLSP-2 with different concentrations on the cell

viability was also evaluated, and the result demonstrated no cytotoxicity at the concentrations studied (Fig. 8B). CLSP-2 significantly inhibited SARS-CoV-2 infection on HeLa cells at ≥12.5 μg/mL with the IC$_{50}$ of 48.48 μg/mL (Fig. 7C, $p < 0.05$). It has been reported that some sulfated polysaccharides, including heparin, fucoidan, and carrageenan, have inhibitory effect against SARS-CoV-2. Due to their negatively charged sulfate groups, these polysaccharides could bind to the S glycoprotein to prevent SARS-CoV-2 host cell entry (Kwon et al., 2020). However, besides sulfation degree, some other structural feathers could affect the anti-virus activity, and some sulfated polysaccharides, such as chondroitin sulfate, showed no obvious inhibitory effects (Song et al., 2020). Of note, CLSP-2 with a sulfate content of 22.7%, which was similar to that of fucoidan, showed stronger anti-SARS-CoV-2 activity than fucoidan. The unique saccharide chain features and highly sulfated substitution of CLSP-2 may contribute to its potential anti-SARS-CoV-2 activity.

4. Conclusions

A novel polysaccharide, CLSP-2 was obtained from edible seaweed *C. lentillifera*. It has a high molecular weight of 3985 kDa, and its morphology was characterized as spherical particles with radii around 200 nm. Its backbone was determined as →6)-β-Man*p*-(1→ branched at C2, and the branch chains were mainly composed of →3)-β-Gal*p*4S-(1→, →3)-β-Gal*p*2,4S-(1→, and minor Xyl. CLSP-2 could prevent HeLa cells from SARS-CoV-2 infection with an IC$_{50}$ of 48.48 μg/mL. The finding in the present study could enlarge the knowledge of *C. lentillifera* resource, and promote its application as the functional ingredients or nutraceuticals in the food and medical industry.

Declaration of competing interest

The authors declare that they have no known competing financial interests or personal relationships that could have appeared to influence the work reported in this paper.

Appendix A. Supplementary data

Supplementary data to this article can be found online at https://doi.org/10.1016/j.carbpol.2021.119006.

References

Alban, S., Schauerte, A., & Franz, G. (2002). Anticoagulant sulfated polysaccharides: Part I. Synthesis and structure-activity relationships of new pullulan sulfates. *Carbohydrate Polymers, 47*(3), 267–276.

Ayerbe, L., Risco, C., & Ayis, S. (2020). The association between treatment with heparin and survival in patients with Covid-19. *Journal of Thrombosis and Thrombolysis, 50* (10229), 298–301.

Fernández, P., Estevez, J. M., Cerezo, A. S., & Ciancia, M. (2012). Sulfated β-D-mannan from green seaweed Codium vermilara. *Carbohydrate Polymers, 87*(1), 916–919.

Hakomori, S. I. (1964). A rapid permethylation of glycolipid, and polysaccharide catalyzed by methylsulfinyl carbanion in dimethyl sulfoxide. *The Journal of Biochemistry, 55*(2), 205–208.

Hans, N., Malik, A., & Naik, S. (2020). Antiviral activity of sulfated polysaccharides from marine algae and its application in combating COVID-19: Mini review. *Bioresource Technology Reports, 13*(6), Article 100623.

Jang, Y., Shin, H., Lee, M. K., Kwon, O. S., Shin, J. S., Kim, Y. I., & Kim, M. (2021). Antiviral activity of lambda-carrageenan against influenza viruses and severe acute respiratory syndrome coronavirus 2. *Scientific Reports, 11*(1), 821.

Kaihou, S., Hayashi, T., Otsuru, O., & Maeda, M. (1993). Studies on the cell-wall mannan of the siphonous green algae, Codium latum. *Carbohydrate Research, 240*, 207–218.

Ken-ichi, Y., Kazuyoshi, I., & Hiroshi. (1997). Structural studies on a sulfated polysaccharide from an Arthrobacter sp. by NMR spectroscopy and methylation analysis. *Carbohydrate Research, 305*(2), 253–260.

Khairuddin, K., Sudirman, S., Huang, L., & Kong, Z.-L. (2020). Caulerpa lentillifera polysaccharides-rich extract reduces oxidative stress and proinflammatory cytokines levels associated with male reproductive functions in diabetic mice. *Applied Sciences-Basel, 10*(24), 8768.

Kwon, P. S., Oh, H., Kwon, S. J., Jin, W., & Dordick, J. S. (2020). Sulfated polysaccharides effectively inhibit SARS-CoV-2 in vitro. *Cell Discovery, 6*(1), 50.

Lu, M. K., Cheng, J. J., Lin, C. Y., & Chang, C. C. (2010). Purification, structural elucidation, and anti-inflammatory effect of a water-soluble 1,6-branched 1,3-α-D-galactan from cultured mycelia of Poria Cocos. *Food Chemistry, 118*(2), 349–356.

Maeda, R., Ida, T., Ihara, H., & Sakamoto, T. (2012). Induction of apoptosis in MCF-7 cells by beta-1,3-xylooligosaccharides prepared from Caulerpa lentillifera. *Bioscience Biotechnology and Biochemistry, 76*(5), 1032–1034.

Needs, P. W., & Selvendran, R. R. (2010). An improved methylation procedure for the analysis of complex polysaccharides including resistant starch and a critique of the factors which lead to undermethylation. *Phytochemical Analysis, 4*(5), 210–216.

Pugh, N., Ross, S. A., Elsohly, H. N., Elsohly, M. A., & Pasco, D. S. (2001). Isolation of three high molecular weight polysaccharide preparations with potent immunostimulatory activity from Spirulina platensis, aphanizomenon flos-aquae and Chlorella pyrenoidosa. *Planta Medica, 67*(08), 737–742.

Song, S., Peng, H., Wang, Q., Liu, Z., Dong, X., Wen, C., & Zhu, B. (2020). Inhibitory activities of marine sulfated polysaccharides against SARS-CoV-2. *Food & Function, 11*(9), 7415–7420.

Song, S., Zhang, B., Wu, S., Huang, L., Ai, C., Pan, J., & Wen, C. (2018). Structural characterization and osteogenic bioactivity of a sulfated polysaccharide from pacific abalone (Haliotis discus hannai Ino). *Carbohydrate Polymers, 182*, 207–214.

Stuthmann, L. E., Springer, K., & Kunzmann, A. (2021). Cultured and packed sea grapes (Caulerpa lentillifera): Effect of different irradiances on photosynthesis. *Journal of Applied Phycology, 33*(2), 1125–1136.

Sun, Y., Gong, G., Guo, Y., Wang, Z., Song, S., Zhu, B., & Jiang, J. (2018). Purification, structural features and immunostimulatory activity of novel polysaccharides from Caulerpa lentillifera. *International Journal of Biological Macromolecules, 108*, 314–323.

Sun, Y., Liu, Y., Ai, C., Song, S., & Chen, X. (2019). Caulerpa lentillifera polysaccharides enhance the immunostimulatory activity in immunosuppressed mice in correlation with modulating gut microbiota. *Food & Function, 10*(7), 4315–4329.

Tanaka, T., Tomii, K., Ueda, T., Kouno, I., & Nakashima, T. (2007). Facile discrimination of aldose enantiomers by reversed-phase HPLC. *Chemical & Pharmaceutical Bulletin, 55*(6), 899–901.

Tian, H., Liu, H., Song, W., Zhu, L., & Yin, X. (2019). Polysaccharide from Caulerpa lentillifera: Extraction optimization with response surface methodology, structure and antioxidant activities. *Natural Product Research, 35*(20), 1–9.

Tuvikene, R., Truus, K., Robal, M., Pehk, T., Kailas, T., Vaher, M., & Paalme, T. (2009). Structure and thermal stability of pyruvated carrageenans from the red alga Coccotylus truncatus. *Carbohydrate Research, 344*(6), 788–794.

Wang, H. X., Zhao, J., Li, D. M., Song, S., Song, L., Fu, Y. H., & Zhang, L. P. (2015). Structural investigation of a uronic acid-containing polysaccharide from abalone by graded acid hydrolysis followed by PMP-HPLC-MSn and NMR analysis. *Carbohydrate Research, 402*, 95–101.

Wang, J., Zhang, Q., Zhang, Z., Hong, Z., & Niu, X. (2010). Structural studies on a novel fucogalactan sulfate extracted from the brown seaweed Laminaria japonica. *International Journal of Biological Macromolecules, 47*(2), 126–131.

Yim, S. K., Kim, K., Kim, I., Chun, S. H., & Jung, K. (2021). Inhibition of SARS-CoV-2 virus entry by the crude polysaccharides of seaweeds and abalone viscera in vitro. *Marine Drugs, 19*(4), 219.

Yun, H., Jing, W., Jin, W., Hong, Z., & Zhang, Q. (2012). Degradation of Laminaria japonica fucoidan by hydrogen peroxide and antioxidant activities of the degradation products of different molecular weights. *Carbohydrate Polymers, 87*(1), 153–159.

Zdorovenko, E. L., Kadykova, A. A., Shashkov, A. S., Varbanets, L. D., Bulyhina, T. V., & Knirel, Y. A. (2017). Lipopolysaccharide of Pantoea agglomerans 7969: Chemical identification, function and biological activity. *Carbohydrate Polymers, 165*, 351.

Zhang, M. J., Ma, Y. R., Che, X. Y., Huang, Z. M., Chen, P., Xia, G. H., & Zhao, M. H. (2020). Comparative analysis of nutrient composition of Caulerpa lentillifera from different regions. *Journal of Ocean University of China, 19*(2), 439–445.